

## Strain effects in chemically lifted GaAs thin films

M. J. Joyce and J. M. Dell

*Telecom Australia Research Laboratories, 770 Blackburn Road, Clayton, Victoria 3168, Australia*

(Received 22 December 1989)

The optical absorption of strained, chemically lifted GaAs films was measured. The films were grown by molecular-beam epitaxy, and then were chemically released from their substrates using a preferential etch and were glued to a quartz plate. Because of the differential thermal expansion of GaAs and quartz, the semiconductor film is under tension below room temperature. From the optical absorption of the film between 10 and 160 K, the hydrostatic and uniaxial deformation potentials were found to be  $a = -7.6 \pm 0.6$  meV and  $b = -1.92 \pm 0.04$  meV, respectively. Very narrow excitonic linewidths were observed at low temperatures, but the exciton-phonon coupling was found to be the same as for an unstrained, bulk GaAs film. The spin-orbit splitting  $\Delta_0$  was found to be independent of temperature between 20 K and room temperature.

### I. INTRODUCTION

The growth of lattice-mismatched epitaxial layers has enabled a wide range of strained semiconductor materials and devices to be fabricated and studied, and has prompted great interest in the effects of strain on these materials. The major rationale for the interest in lattice-mismatched material systems has been the desire to combine the properties of two (or more) disparate materials for a single electronic or optoelectronic device. This has resulted in the recent development of, for example, the GaAs/Si,<sup>1</sup> GaAs/InP,<sup>2</sup> and  $\text{In}_x\text{Ga}_{1-x}\text{As}/\text{GaAs}$  (Ref. 3) lattice-mismatched systems. Recently, much interest has centered on the selective chemical release of epitaxially grown material from its substrate.<sup>4-7</sup> This technique opens up significant new areas for materials research and device fabrication<sup>5-7</sup> and may provide a novel and technologically useful method for combining lattice-mismatched materials.

Recently, we reported<sup>8</sup> the near band-gap optical absorption of a chemically released GaAs film on a quartz substrate. It was shown that the optical properties of the epitaxial films were not degraded by the liftoff process, as evidenced by strong excitonic absorption features that persisted even to room temperature. Due to the differential thermal expansion coefficients of GaAs and the much thicker quartz substrate, the semiconductor layer is under tension at temperatures below room temperature. Varying the sample temperature therefore provides a simple technique for investigating the effects of strain in GaAs.

The valence band of GaAs at the center of the Brillouin zone consists of a fourfold-degenerate multiplet ( $J = \frac{3}{2}$ ,  $m_j = \pm \frac{3}{2}, \pm \frac{1}{2}$ ) and a spin-orbit-split doublet state ( $J = \frac{1}{2}$ ,  $m_j = \pm \frac{1}{2}$ ).<sup>9,10</sup> If the material is uniaxially or biaxially strained, the degeneracy of the  $J = \frac{3}{2}$  multiplet is raised and it splits into  $m_j = \pm \frac{3}{2}$  ["heavy" hole (HH)] and  $m_j = \pm \frac{1}{2}$  ["light" hole (LH)] bands. We were able to observe both electron-to-LH and electron-to-HH absorption, as well as electron to spin-orbit-split transitions in

the transmission spectra of the thin GaAs film.

The strong, narrow absorption peaks exhibited by these thin films allow the excitonic positions to be accurately found. We were able, therefore, to determine the hydrostatic and uniaxial deformation potentials of GaAs at temperatures between 10 and 160 K and could also measure the spin-orbit splitting up to room temperature. The linewidth of the heavy-hole exciton was found to broaden with increasing temperature due to exciton-phonon coupling, with the strength of the coupling being in agreement with earlier measurements.

### II. EXPERIMENTAL

The preparation of a GaAs thin film on a quartz substrate has been described in detail previously<sup>4,8</sup> and will only be outlined here. On a (100)-oriented, semi-insulating GaAs substrate, a 0.4- $\mu\text{m}$  undoped GaAs buffer layer was grown using molecular-beam epitaxy (MBE), followed by a 500- $\text{\AA}$  AlAs release layer and then 1.3  $\mu\text{m}$  of undoped GaAs. After the growth, 4 $\times$ 4-mm squares of material were coated with "Apiezon W" wax, and the AlAs layer was selectively removed using a 10% HF etch at a temperature a few degrees below 0°C. The lifted-off GaAs layer was then bonded to a quartz substrate using uv-cured Norland optical adhesive No. 81. Finally, the wax was removed with trichloroethylene.

For the transmission measurements, mechanically chopped light from a tungsten lamp was passed through a 1-m Chromatix monochromator and focused onto the sample. The transmitted light was detected using either a Si *p-i-n* detector or a room-temperature GaAs photomultiplier tube (PMT), in conjunction with a lock-in amplifier. The sample was mounted film side down on the cold finger of a closed-cycle He cryostat, the temperature of which could be varied from 10 to 300 K. To ensure that good thermal contact was maintained between the GaAs and the cold finger, the two were held together by a slight force applied by springs on the back of the quartz substrate. The temperature was monitored with two Chromel/gold thermocouples, one on the copper

mount and one on the back of the quartz. These agreed to within 1.5 K at all temperatures. Transmission was measured through a 0.5-mm aperture in the cold finger, with care being taken to prevent stray light by-passing the sample and reaching the detector.

Three different transmission measurements were made to verify that there was no stress on the GaAs due to contact with the copper mount. Firstly, a spectrum was measured with the sample mounted in the cryostat; secondly, the sample and the copper mount were removed from the cryostat and immersed in liquid nitrogen. Finally, the sample was loosely held in liquid nitrogen. In each case the spectra were identical in terms of the strength, linewidth, and energy position of the features.

In addition to absorption measurements, phototransmission (PT)<sup>11</sup> was also employed to characterize this material, using the experimental arrangement shown in Fig. 1. This technique is similar to the better known photoreflexion (PR) technique.<sup>12,13</sup> White light is passed through the monochromator and an order-separating filter and focused onto the sample. The 515-nm light from an argon ion laser is chopped and  $\sim 5 \text{ mW/cm}^2$  is also directed onto the sample. A long pass filter was used to block the laser light from the Si *p-i-n* detector used in these measurements. The signal at the detector consists of an unmodulated component (the transmission spectrum) and a modulated component, made up<sup>13</sup> of PT and photoluminescence (PL). This latter component, which becomes dominant at low temperatures, appears at the detector as a wavelength-independent modulated background and so can be subtracted from the PT. At 10 K, this PL was so strong, however, that the weaker PT signal could not be determined at all. The final spectrum is obtained by normalizing the PT to the (unmodulated) transmission spectrum.

To determine the unstrained band gap of GaAs as a

function of temperature, we analyzed another sample of GaAs that had been grown at the same time as the lifted-off sample. As this layer was not removed from its substrate, it remained unstrained at all temperatures. Transmission measurements could not be used to characterize this sample (because of the substrate), so the band edge was measured using reflection, photoreflexion, and photoluminescence spectroscopies. The PR was measured using a similar arrangement to that of Fig. 1, and the PL was measured using the argon ion laser and the GaAs PMT.

### III. RESULTS AND ANALYSIS

The differential thermal expansions of the quartz substrate and the GaAs film causes the latter to be under tension at temperatures below room temperature. The known expansion coefficients for the two materials<sup>14,15</sup> can be used to determine the (positive) biaxial strain at a given temperature via

$$\epsilon(T) = \int_{295 \text{ K}}^T [\alpha_{\text{GaAs}}(T') - \alpha_{\text{quartz}}(T')] dT', \quad (1)$$

where  $\epsilon$  is the strain,  $T$  the temperature, and  $\alpha$  the expansion coefficient. This strain is shown in Fig. 2 and can be seen to reach a maximum value of about  $10^{-3}$  at 0 K, equivalent to an external pressure of  $\sim 0.8 \text{ kbar}$ . The biaxial tension in the GaAs film causes a corresponding compression in the direction perpendicular to the layer. The total strain can be regarded as being made up of a hydrostatic component and a uniaxial component acting in the perpendicular direction. The direct energy gaps at  $\Gamma$  are altered by the strain as follows:<sup>9,10</sup>

$$E_0^{e\text{-HH}}(\epsilon, T) = E_0(T) + \delta E_H - \delta E_U, \quad (2)$$

$$E_0^{e\text{-LH}}(\epsilon, T) = E_0(T) + \delta E_H + \delta E_U - 2\delta E_U^2/\Delta_0, \quad (3)$$

$$E_0^{e\text{-SS}}(\epsilon, T) = E_0(T) + \delta E'_H + \Delta_0 + 2\delta E_U^2/\Delta_0, \quad (4)$$

where  $E_0^{e\text{-LH}}(\epsilon, T)$  is the energy of the electron-to-

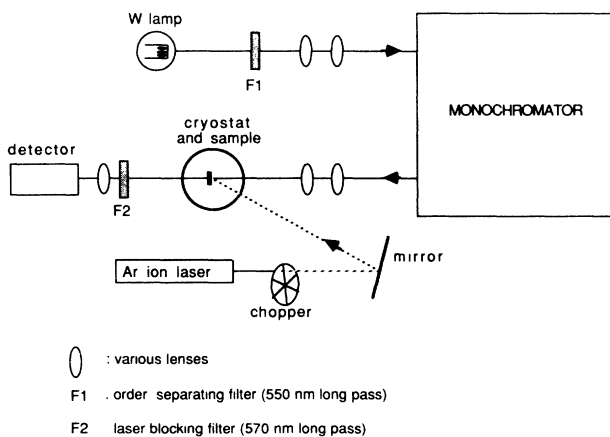


FIG. 1. Schematic view of the experimental arrangement for observing phototransmission (PT) spectroscopy. Similar arrangements were used to measure transmission and photoreflexion (PR) spectra.

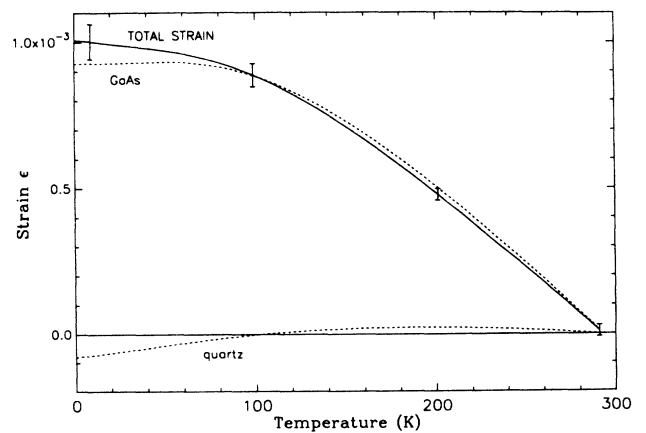


FIG. 2. Calculated strain in a GaAs thin film on a quartz substrate. The dashed curves show the thermal contraction of freely suspended GaAs (Ref. 14) and quartz (Ref. 15), while the solid line shows the biaxial strain induced in a GaAs film constrained by quartz. Error bars refer to total strain.

(light-) heavy-hole band gap, and  $E_0^{\epsilon\text{-SS}}(\epsilon, T)$  the energy of the electron-to-spin-split-hole band gap as a function of strain,  $\epsilon$ , and temperature  $T$ .  $E_0(T)$  is the unstrained band gap of GaAs,

$$\delta E_H = 2a \left( \frac{C_{11} - C_{12}}{C_{11}} \right) \epsilon \quad (5)$$

and

$$\delta E_H' = 2a' \left( \frac{C_{11} - C_{12}}{C_{11}} \right) \epsilon \quad (5')$$

are the hydrostatic strain shifts of the energy gap (which, for  $\epsilon > 0$ , result in a decrease in the gap), and

$$\delta E_U = b \left( \frac{C_{11} + 2C_{12}}{C_{12}} \right) \epsilon \quad (6)$$

is the uniaxial contribution to the energy shifts (which splits the HH-LH degeneracy, with the light-hole band moving to higher energy than the heavy-hole band under tensile strain).  $C_{11}$  and  $C_{12}$  are the elastic constants and  $a$  and  $b$  are the hydrostatic and uniaxial deformation potentials, respectively. The elastic constants have a small temperature dependence, which is assumed to be linear.<sup>16</sup> The hydrostatic deformation potential is related to the pressure derivative of the band edge (under hydrostatic strain) by

$$a = -B_0 \partial E_0 / \partial P, \quad (7)$$

where  $B_0 = (C_{11} + 2C_{12})/3$  is the bulk modulus.  $\Delta_0$  is the splitting at  $\Gamma$  between the degenerate LH and HH bands and the spin-orbit-split-hole band at zero strain, and is taken to be 341 meV.<sup>17</sup> The final term in Eqs. (3) and (4) accounts for the interaction between the light hole and the split-off hole, which causes the two bands to move apart from each other as  $|\epsilon|$  increases.

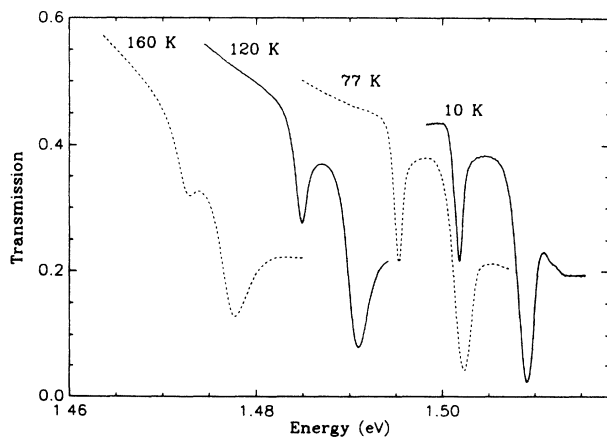


FIG. 3. Transmission of a 1.3- $\mu\text{m}$  GaAs film on a quartz substrate, measured as a function of temperature. The light-hole and heavy-hole excitons are split by the biaxial strain in the thin film, with the light hole shifting to a lower energy than the heavy hole.

Transmission measurements in these strained thin films yield spectra with strong, sharp excitonic features,<sup>8</sup> as shown in Fig. 3. From the observed splitting of the LH and HH absorption peaks as a function of temperature, the uniaxial deformation potential  $b$  can be determined. Using the strain from Fig. 2, the splitting is fitted very well with  $b = -1.92 \pm 0.04$  meV, as shown in Fig. 4. In obtaining this result, we have assumed that the LH and HH exciton binding energies are equal. Above 160 K, the splitting cannot be obtained from our spectra since it is too small and the linewidths are too large to resolve it. The value of  $b$  obtained is constant over the temperature range considered and is in good agreement with measurements of other workers made at fixed temperatures. A comparison with some of these previous measurements is shown in Table I.

To determine the hydrostatic deformation potential  $a$ , the unstrained band gap  $E_0$  was determined as a function of temperature. As already described, an unstrained sample of GaAs was analyzed using reflection, PR, and PL spectroscopies. In Fig. 5 representative data for the reflectance  $R$ , its (calculated) logarithmic derivative  $(1/R)(dR/dE)$ , and the PR signal at 100 K are shown. The PR signal is fitted with a third derivative functional form<sup>12</sup> and the position of the two significant features is marked with vertical arrows. One feature arises from the exciton and the other is due to the band edge, the latter being  $\sim 4$  meV—an exciton Rydberg—higher in energy. It can be seen that the strong dip in the  $(1/R)(dR/dE)$  spectrum<sup>18</sup> is very close in energy to the exciton position found by PR. This was so for spectra at all temperatures above about 50 K. Below this temperature, the PR signal is more difficult to measure, since PL is also present at the detector, and it was found that the two techniques differed by up to 2 meV. The dip in the reflectance derivative was taken to be a more accurate measure of the band edge below 50 K. PL spectra were measured at temperatures up to 160 K and the variation of the peak

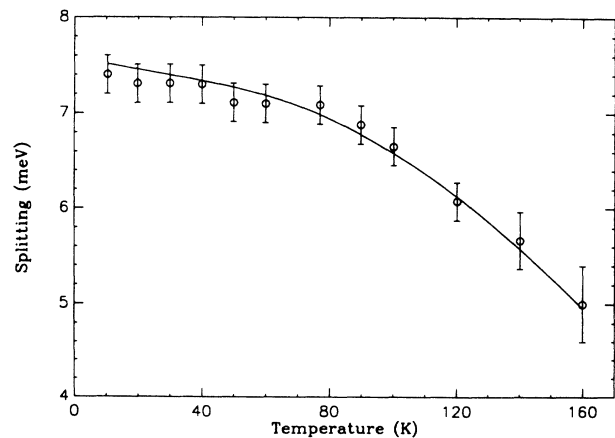


FIG. 4. Observed and calculated light-hole-heavy-hole splitting as a function of temperature. The solid curve was calculated using Eqs. (1)–(6), assuming a temperature-independent uniaxial deformation potential  $b = -1.92$  meV. The data points were determined from transmission spectra.

TABLE I. Hydrostatic ( $a$ ) and uniaxial ( $b$ ) deformation potentials for GaAs at various temperatures. The values from this work were determined over the temperature range indicated, with the sample under a small biaxial tension. (RT denotes room temperature.)

| Temperature | $a$ (meV)         | $b$ (meV)          |
|-------------|-------------------|--------------------|
| 20–160 K    | $-7.6 \pm 0.6^a$  | $-1.92 \pm 0.04^a$ |
| RT          | $-8.1 \pm 0.03^b$ | $-1.7 \pm 0.2^b$   |
|             | $-9.0 \pm 0.4^c$  | $-2.0 \pm 0.2^c$   |
|             | $-8.7 \pm 0.2^d$  |                    |
|             | $-9.1 \pm 1^e$    |                    |
|             | $-9.3^f$          |                    |
| 150 K       | $-8.5 \pm 0.1^g$  |                    |
| 120 K       | $-7.4^f$          |                    |
| 77 K        | $-8.8 \pm 0.03^b$ | $-1.7 \pm 0.2^b$   |
|             | $-8.7 \pm 1^h$    | $-1.7 \pm 0.1^h$   |
|             | $-8.5 \pm 0.1^g$  |                    |
|             | $-8.4^i$          |                    |
| 8 K         | $-8.5 \pm 0.1^g$  |                    |
| 5 K         | $-8.5 \pm 0.5^j$  |                    |
| 2 K         | $-9.1 \pm 0.5^k$  | $-1.96 \pm 0.1^k$  |

<sup>a</sup>This work.

<sup>g</sup>Reference 28.

<sup>b</sup>Reference 23.

<sup>h</sup>Reference 9.

<sup>c</sup>Reference 24.

<sup>i</sup>Reference 29.

<sup>d</sup>Reference 25.

<sup>j</sup>Reference 30.

<sup>e</sup>Reference 26.

<sup>k</sup>Reference 31.

<sup>f</sup>Reference 27.

position with temperature agreed with the temperature variation of the reflectance dip.

The measured position of the exciton as a function of temperature was fitted with a fourth-order polynomial to allow smooth interpolation of the data. The uncertainty in the band edge is estimated to be  $\pm 0.5$  meV. Using our value of the deformation potential  $b = -1.92$  meV, the position of the strained light- and heavy-hole excitons observed in absorption could be fitted with a temperature-independent hydrostatic deformation potential  $a = -7.6$

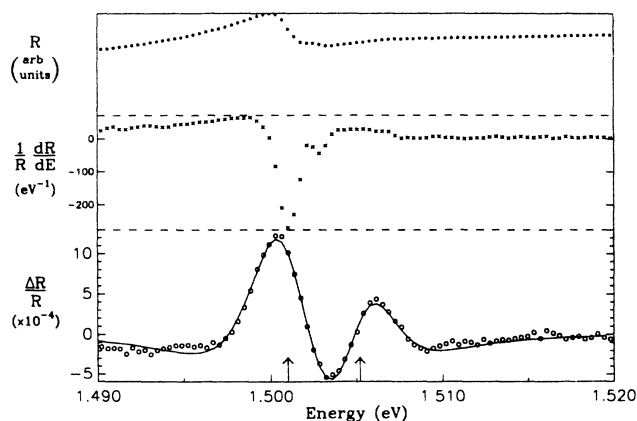


FIG. 5. The reflectance  $R$ , its (calculated) logarithmic derivative  $(1/R)(dR/dE)$ , and the PR spectrum of unstrained GaAs at 100 K. Circles and crosses represent experimental points, while the solid line is a fit to the PR using a third derivative functional form (Ref. 12), with an exponent of  $-3$ . The arrows show the energy positions of the band edge and exciton found from the PR fitting procedure.

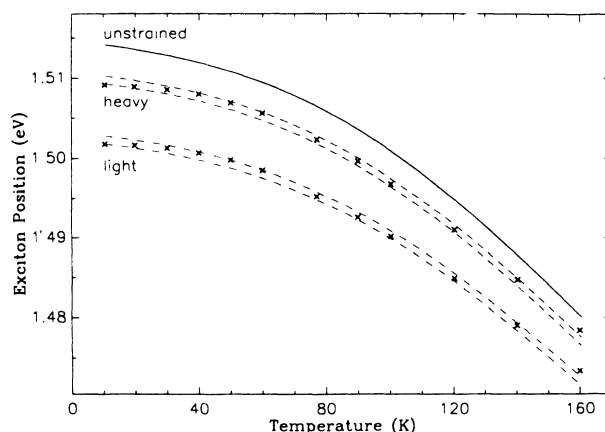


FIG. 6. Observed and calculated strained exciton position as a function of temperature. The unstrained excitonic position was determined from reflectance measurements. The dot-dashed (dashed) curves represent the calculated heavy- (light-) hole exciton position assuming  $a = -7.6$  meV and  $b = -1.92$  meV and an uncertainty of  $\pm 0.5$  meV arising from the uncertainty in the unstrained exciton position (solid line). The error in the measured points (crosses) is only  $\sim \pm 0.1$  to  $\pm 0.2$  meV and so is not visible on this scale.

meV up to 160 K, as shown in Fig. 6. An uncertainty of  $\pm 0.6$  meV in the calculated value of  $a$  is estimated, due mainly to the  $\pm 0.5$ -meV uncertainty in the unstrained band gap, and also to the smaller uncertainty ( $\sim \pm 0.1$  to  $\pm 0.2$  meV) in the strained exciton positions. This value of  $a$  is in good agreement with previous values, measured at both lower and higher temperatures, as shown in Table I. This is believed to be the first measurement of the strain deformation potentials of GaAs with the material in tension, and also the first over a wide, continuous temperature range. It shows that both  $a$  and  $b$  are temperature independent up to 160 K.

The spin-split hole was observable in both transmission

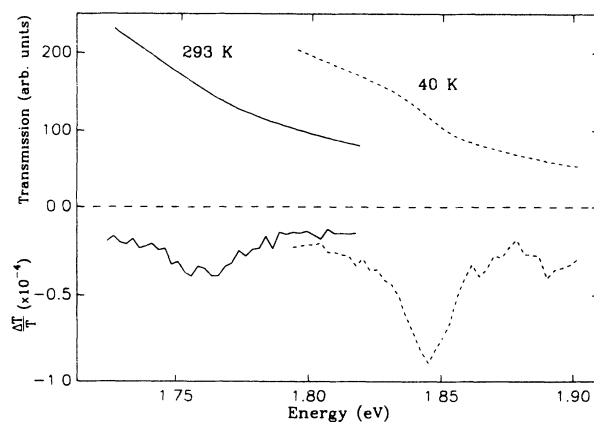


FIG. 7. The spin-split hole in the GaAs thin film on quartz, as observed with transmission and phototransmission (PT) spectroscopy. PT allows the spin-split hole position to be determined to within a few meV, even though the feature in the transmission spectrum is very broad.

and PT spectra, as shown in Fig. 7. PT allows us to determine the energy of this transition to within a few meV up to room temperature, even though the feature in the transmission spectrum is very broad. The PT feature was fitted with a similar line shape to the PR as described above. It was found that the energy difference between this feature and the average position of the light- and heavy-hole excitons was  $340.5 \pm 3$  meV at all temperatures, as shown in Fig. 8. It is expected from Eqs. (2)–(6) that the spin-orbit splitting will be independent of strain and temperature if  $\Delta_0$  is temperature independent and the deformation potentials  $a$  and  $a'$  are equal. The two deformation potentials have been estimated<sup>9</sup> to differ by less than 1%, and since  $\delta E'_H$  is much smaller than  $\Delta_0$ , the effect of this small difference is negligible for the small strains present in our experiment. Our result therefore indicates that the spin-orbit splitting is temperature independent from 20 K up to room temperature. The actual value of  $\Delta_0$  depends upon whether the observed spin-split feature arises due to excitonic or band-edge absorption. In the former case, assuming a split-off exciton binding energy of 3.4 meV,<sup>17</sup> we find  $\Delta_0 = 340 \pm 3$  meV. In the latter case,  $\Delta_0$  will be  $336 \pm 3$  meV. A previous measurement of the spin-orbit splitting over this temperature range<sup>19</sup> also indicated that  $\Delta_0$  is temperature independent, with a value of 350 meV. Measurements made by others at room temperature<sup>20</sup> and 4 K (Ref. 17) give values of 340 and 341 meV, respectively. Our results are clearly in excellent agreement with Refs. 17 and 20 and confirm the temperature independence of  $\Delta_0$  over the entire temperature range of 20 to 300 K.

Finally, an analysis of the linewidths of the transmission peaks is of interest. Using the technique described elsewhere,<sup>8</sup> the transmission spectra are converted to absorption and the linewidth [full width at half maximum (FWHM)] of the heavy- and light-hole excitonic peaks

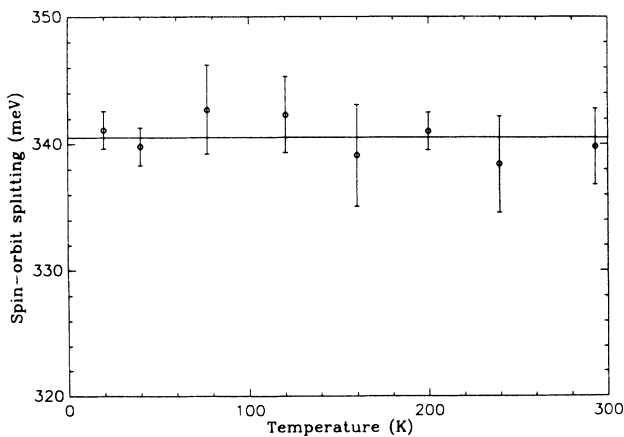


FIG. 8. The energy difference between the spin-split feature observed in PT (see Fig. 7) and the average position of the light-hole and heavy-hole exciton in the strained GaAs thin film. This energy difference is  $340.5 \pm 3$  meV over the temperature range shown.

can be determined using a fitting technique. The excitonic absorption is fitted with Gaussian peaks, and the band edge is modeled semi-empirically as a broadened continuum.<sup>21</sup> For the light-hole exciton, the linewidth could only be determined at the lowest temperatures and was found to be  $0.9 \pm 0.1$  meV, as shown in Fig. 9. This figure also shows the HH linewidth as a function of temperature up to room temperature. The HH linewidth broadening as a function of temperature is found to be matched very well by a model of exciton scattering from longitudinal optical (LO) phonons. The linewidth is made up of a low temperature value  $\Gamma_0$ , and a term due to the scattering,<sup>21</sup>

$$\Gamma(T) = \Gamma_0 + \Gamma_{\text{ph}}[\exp(E_{\text{ph}}/kT) - 1]^{-1}, \quad (8)$$

where  $E_{\text{ph}}$  is the LO-phonon energy and is 36 meV for GaAs,  $kT$  is the thermal energy, and  $\Gamma_{\text{ph}}$  is a measure of the exciton-phonon coupling. A good fit is obtained with  $\Gamma_0 = 1.3 \pm 0.1$  meV and  $\Gamma_{\text{ph}} = 14$  meV for the heavy hole, as shown. For the light hole,  $\Gamma_0$  is 0.9 meV, but  $\Gamma_{\text{ph}}$  appears to be smaller than the 14 meV observed for the heavy hole.  $\Gamma_0$  compares very favorably with previous measurements,<sup>21,22</sup> indicating the high quality of this material. The strength of the exciton-phonon coupling  $\Gamma_{\text{ph}}$  in our thin film agrees exactly with an earlier measurement on bulk, unstrained GaAs (Ref. 22) but is smaller than measurements of the coupling in a GaAs/AlGaAs multiple quantum well<sup>21</sup> (11 meV).

In summary, we have studied strain effects in a chemically released GaAs thin film using absorption and reflection spectroscopies. The strong, sharp excitonic features observed allowed determination of the hydrostatic and uniaxial deformation potentials, which were shown to be independent of temperature up to 160 K. The

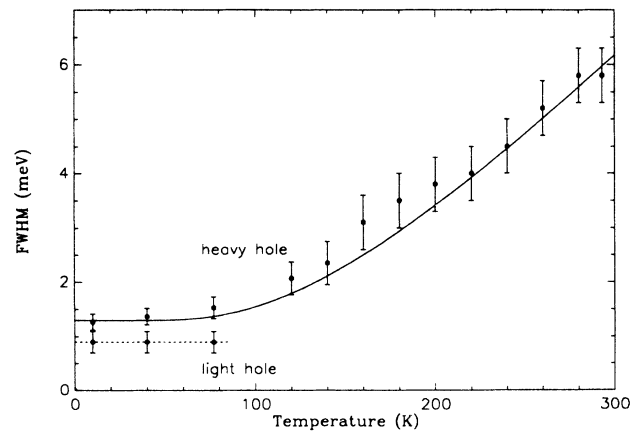


FIG. 9. The measured full width at half maximum (FWHM) of the light-hole and heavy-hole excitons as a function of temperature. The solid line is a fit to Eq. (8) with  $\Gamma_0 = 1.3$  meV and  $\Gamma_{\text{ph}} = 14$  meV and shows that the heavy-hole broadening is well described by a model of exciton scattering. The light-hole FWHM could only be determined up to 77 K.

spin-orbit splitting  $\Delta_0$  was shown to be temperature independent up to room temperature, and the heavy-hole linewidth was shown to broaden with temperature due to exciton-phonon coupling, with a coupling strength identical to unstrained GaAs.

#### ACKNOWLEDGMENTS

The permission of the executive general manager of Telecom Research Laboratories to publish this paper is hereby acknowledged.

- <sup>1</sup>R. Fischer, H. Morkoç, D. A. Neumann, H. Zabel, C. Choi, N. Otsuka, M. Longebone, and L. P. Erickson, *J. Appl. Phys.* **60**, 1640 (1986).
- <sup>2</sup>K. Asano, K. Kasahara, and Tomohiro Itoh, *IEEE Electron Devices Lett.* **EDL-8**, 289 (1987).
- <sup>3</sup>S. E. Fischer, R. G. Waters, D. Fekete, J. M. Ballantyne, Y. C. Chen, and B. A. Soltz, *Appl. Phys. Lett.* **54**, 1861 (1989).
- <sup>4</sup>E. Yablonovitch, T. J. Gmitter, J. P. Harbison, and R. Bhat, *Appl. Phys. Lett.* **51**, 2222 (1987).
- <sup>5</sup>E. Yablonovitch, K. Kash, T. J. Gmitter, L. T. Florez, J. P. Harbison, and E. Colas, *Electron. Lett.* **25**, 171 (1989).
- <sup>6</sup>E. Yablonovitch, E. Kapon, T. J. Gmitter, C. P. Yun, and R. Bhat, *Phot. Tech. Lett.* **1**, 41 (1989).
- <sup>7</sup>J. F. Klem, E. D. Jones, D. R. Myers, and J. A. Lott, *J. Appl. Phys.* **66**, 459 (1989).
- <sup>8</sup>J. M. Dell, M. J. Joyce, B. F. Usher, G. W. Yoffe, and P. C. Kemeny (unpublished).
- <sup>9</sup>M. Chandrasekhar and F. H. Pollak, *Phys. Rev. B* **15**, 2127 (1977).
- <sup>10</sup>D. A. Dahl, *Solid State Commun.* **61**, 825 (1987).
- <sup>11</sup>C. Van Hoof, D. J. Arent, K. Deneffe, J. DeBoeck, and G. Borghs, *J. Appl. Phys.* **64**, 4233 (1988).
- <sup>12</sup>U. K. Reddy, G. Ji, T. Henderson, H. Morkoç, and J. N. Schulman, *J. Appl. Phys.* **62**, 145 (1987).
- <sup>13</sup>X. L. Zheng, D. Heiman, B. Lax, and F. A. Chambers, *Superlattices and Microstructures* **4**, 351 (1988).
- <sup>14</sup>*Landolt-Börnstein, Numerical Data and Functional Relationships in Science and Technology*, edited by O. Madelung (Springer, Berlin, 1982), Gp. III, Vol. 17a.
- <sup>15</sup>R. J. Corruccini and J. J. Gniewek, *Thermal Expansion of Technical Solids at Low Temperatures*, National Bureau of Standards Monograph No. 29 (U.S. GPO, Washington, D.C., 1961).
- <sup>16</sup>We use  $C_{11} = 11.88 - 0.00148 \times [300 - T \text{ (K)}]$  and  $C_{12} = 5.38 - 0.00126 \times [300 - T \text{ (K)}]$ . The end-point values are taken from Ref. 14.
- <sup>17</sup>D. E. Aspnes and A. A. Studna, *Phys. Rev. B* **7**, 4605 (1973).
- <sup>18</sup>D. D. Sell, H. C. Casey Jr., and K. W. Wecht, *J. Appl. Phys.* **45**, 2650 (1974).
- <sup>19</sup>T. Nishino, M. Okuyama, and Y. Hamakawa, *J. Phys. Chem. Solids* **30**, 2671 (1969).
- <sup>20</sup>E. W. Williams and V. Rehn, *Phys. Rev.* **172**, 798 (1968); A. G. Thompson, M. Cardona, K. L. Skaklee, and J. C. Woolley, *ibid.* **146**, 601 (1966).
- <sup>21</sup>D. S. Chemla, D. A. B. Miller, P. W. Smith, A. C. Gossard, and W. Wiegmann, *IEEE J. Quantum Electron.* **QE-20**, 265 (1984).
- <sup>22</sup>V. L. Alperovich, V. M. Zaletin, A. F. Kravchenko, and A. S. Terekhov, *Phys. Status Solidi B* **77**, 465 (1976).
- <sup>23</sup>J. Feinleib, S. Groves, W. Paul, and R. Zallen, *Phys. Rev.* **131**, 2070 (1963).
- <sup>24</sup>F. H. Pollak and M. Cardona, *Phys. Rev.* **172**, 816 (1968).
- <sup>25</sup>R. Bendorius and A. Shileika, *Solid State Commun.* **8**, 1111 (1970).
- <sup>26</sup>J. Wajda and M. Grynberg, *Phys. Status Solidi* **37**, K55 (1970).
- <sup>27</sup>D. Olego, M. Cardona, and H. Müller, *Phys. Rev. B* **22**, 894 (1980).
- <sup>28</sup>U. Venkateswaran *et al.*, *Superlatt. Microstruct.* **3**, 217 (1987).
- <sup>29</sup>T. Kobayashi, *J. Soc. Mater. Sci. Jpn.* **413**, 132 (1988).
- <sup>30</sup>D. J. Wolford and J. A. Bradley, *Solid State Commun.* **53**, 1069 (1985).
- <sup>31</sup>R. N. Bhargava and M. Nathan, *Phys. Rev.* **161**, 695 (1967).

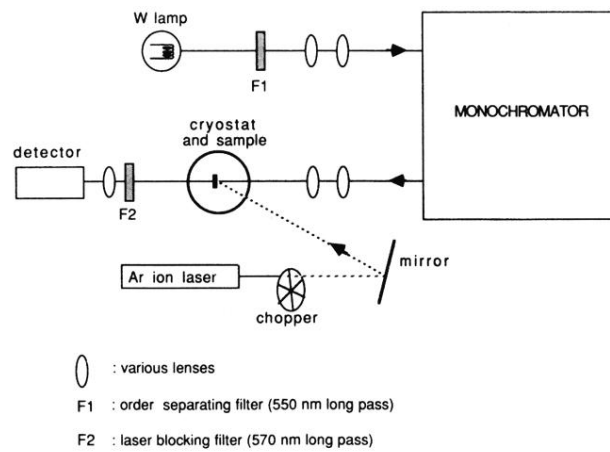


FIG. 1. Schematic view of the experimental arrangement for observing phototransmission (PT) spectroscopy. Similar arrangements were used to measure transmission and photoreflectance (PR) spectra.